Can Swiss wheat varieties escape future heat stress?

European Journal of Agronomy 131 (2021) 126394

Contents lists available at ScienceDirect

European Journal of Agronomy

journal homepage: www.elsevier.com/locate/eja

Can Swiss wheat varieties escape future heat stress?

Julian Rogger [a,*], Andreas Hund [b], Dario Fossati [c], Annelie Holzkämper [a,d]

[a] Agroscope, Group of Climate and Agriculture, Division of Agroecology and Environment, Zürich, Switzerland
[b] ETH Zürich, Group of Crop Science, Department of Environmental Systems Science, Zürich, Switzerland
[c] Agroscope, Group of Plant Breeding, Division of Plant Production Sciences, Nyon, Switzerland
[d] University of Bern, Oeschger Centre for Climate Change Research, Bern, Switzerland

ARTICLE INFO

Keywords:
Wheat
Switzerland
Climate change adaption
Phenology
Heat stress
Heat escape

ABSTRACT

Climate change-induced heat waves represent a severe threat to future global crop production. The extent of heat stress for agricultural crops depends on the co-occurrence of heat periods and heat sensitive phenological stages. Using the Wang and Engel phenology model and the most recent climate change projections for four sites across the Swiss Central Plateau, we estimated future heat stress exposure in Swiss wheat production and tested the potential of winter wheat genotypes with differing phenological characteristics to escape future heat periods. Across all genotypes, heat stress days ($T_{max} \geq 30$ °C) during the temperature sensitive stages of flowering and early grain filling increased from an average of 1.5 heat days in 1982–2006 to 2.1 by 2075–2099 with RCP2.6 (with climate change mitigation) and to 3.6 by 2075–2099 with RCP8.5 (without climate change mitigation), respectively. Across all genotypes and locations, a considerable escape from future heat periods was modelled due to a mainly temperature-driven advancement in the phenological development. Under both RCP scenarios, we predicted lower exposure to heat stress for early varieties than for late varieties. However, under the RCP8.5 scenario, for each location, heat stress exposure for early varieties was still projected to be higher by 2075–2099 than for late varieties under current conditions. Further, heat stress exposure was considerably increased at locations with cooler spring conditions, slowing down the early season phenological development and resulting in late heading dates. Our findings imply needs for a regionally adequate cultivar selection as well as for phenological adaptions and heat tolerance traits in Swiss wheat breeding to adapt to future climate change and regional climatic differences. Different strategies of breeding adaptations and their trade-offs are discussed.

1. Introduction

With an annual production of more than 700 million tons (www.fao.org/faostat), wheat ranks among the most important food crops for human consumption. However, global wheat production is heavily challenged by the consequences of anthropogenic climate change. Lobell et al. (2011) attributed a 5.5 % decline in global wheat yields from 1980 to 2008 to climate change driven shifts in temperature and precipitation. Similarly, using a multi-model ensemble of 30 crop models, wheat grain yields were predicted to decrease by 6 % per 1 °C increase of the Earth's surface temperature, accompanied by an increasing spatial and temporal yield variability (Asseng et al., 2015). More frequent heat waves during temperature sensitive phenology stages are thereby expected to add considerably to global crop yield variability (IPCC, 2019). In Europe, such heat waves are expected to become more intense, frequent and extended in duration throughout the 21st century (Meehl and Tebaldi, 2004; Schär et al., 2004; Seneviratne et al., 2006).

Regarding wheat production, large concern is given to heat events occurring during the reproductive growth between heading and plant maturity, the period when the crop is especially sensitive to extreme temperatures (Entz and Fowler, 1988). Following heading and during subsequent anthesis, heat events can result in a large proportion of sterile pollen and infertile florets, reduce the number of grains and induce grain deformations (e.g., small, notched, shriveled or split grains). During grain filling, high temperatures trigger premature senescence, decreased leaf chlorophyll and hinder kernel development due to an inhibited photosynthate translocation to the developing grain. All these heat-induced physiological impacts considerably reduce yields and grain quality, as reviewed by Porter and Gawith (1999), Farooq et al. (2011) and Barlow et al. (2015). Given the same 'heat load', heat events during grain filling are more devasting than just an increased average temperature (Wardlaw et al., 2002).

* Corresponding author.
E-mail address: julian.rogger@erdw.ethz.ch (J. Rogger).

https://doi.org/10.1016/j.eja.2021.126394
Received 13 March 2021; Received in revised form 26 July 2021; Accepted 8 September 2021
Available online 21 September 2021

Yield losses due to such heat events were already reported for several regions of the world (Brisson et al., 2010; Kristensen et al., 2011; Liu et al., 2014). Moreover, heat stress was modelled to further increase for major global wheat production regions, especially during the second half of the 21st century (Gouache et al., 2012; Semenov, 2009; Semenov and Shewry, 2011; Semenov et al., 2014; Stratonovitch and Semenov, 2015; Strer et al., 2018; Trnka et al., 2014; Wang et al., 2015). Also for Switzerland, the region of interest in the present study, heat stress during grain filling was identified as a main source of abiotic stress for winter wheat throughout the last decades and is expected to remain important under climate change (Holzkämper et al., 2014). For the Swiss Plateau, the country's main wheat production region, more than 30 hot days (temperatures $\geq$30 °C) per year are expected towards the end of the 21st century under a high greenhouse gas (GHG) emission scenario (CH2018, 2018). Yet so far, estimations of heat stress occurrence in Swiss wheat production under climate change have not been conducted.

The extent of heat damage to the crop depends on the co-occurrence of critical heat periods and sensitive phenological stages. Thereby, the exact timing of these stages shifts as a function of growing season temperatures. Increasing average temperatures were observed to advance the phenology of wheat and other annual agricultural crops in several regions of the world (Estrella et al., 2007; He et al., 2015; Ren et al., 2019; Rezaei et al., 2018; Tao et al., 2012). This effect is also expected to occur in Switzerland (Torriani et al., 2007), considering that the observed warming rate of the near-surface temperature in Switzerland is more than double the global average (2 °C vs. 0.9 °C during 1864–2016) (CH2018, 2018). A warming-induced advancement of wheat phenology was proposed to potentially offset the effects of more frequent heat periods under climate change by escaping high maximum temperatures towards summer (Rezaei et al., 2015). Accordingly, adjusting the crop calendar towards early heading and maturing varieties is an often discussed climate change adaption measure to escape future heat stress (Gouache et al., 2012; Mondal et al., 2016; Trnka et al., 2014). In fact, in Germany the advancement in wheat phenology was shown to be due to both, rising growing season temperatures as well as the adoption of earlier varieties (Rezaei et al., 2018). Similar trends can be expected for Switzerland. However, it is not clear if and to what extend the mechanism of phenological heat escape will continue to prevent heat stress exposure of winter wheat with progressing global warming. It is also not clear to what extend phenological differences of currently cultivated varieties allow for a reduction in heat stress exposure.

It is therefore the aim of this study to explore the possibilities of Swiss winter wheat varieties to escape from heat stress during critical phenological phases under climate change. For this purpose, we parametrized the Wang and Engel phenology model (Wang and Engel, 1998) for a selected set of wheat varieties representative of the currently observed spectrum of phenological development rates in Swiss wheat production. Further, using the recent downscaled climate change projections, heading dates and indicators of heat stress occurrence were modelled throughout the 21st century. This approach allowed us to quantify (i) phenological shifts to be expected with future climate change until the end of the century, and (ii) future heat stress exposure of winter wheat varieties currently cultivated in Switzerland. With that, we assess the possibility to reduce future heat stress exposure through phenological advancement and genotypic earliness within the range of cultivars grown in Switzerland today.

2. Materials and methods

2.1. Phenology model

The used Wang and Engel cereal phenology model (Wang and Engel, 1998) was assessed to predict genotype specific phenological development with good accuracy (Aslam et al., 2017; Streck et al., 2003b; Wang and Engel, 1998; Wu et al., 2017; Xue et al., 2004). It is a non-linear multiplicative model in which the daily phenological development rate of a cereal plant is described by a maximum development rate R_{max}, a vernalization response function $f(V)$, a temperature response function $f(T)$ and a photoperiod response function $f(P)$ according to:

$$r\left[d^{-1}\right] = R_{\max}\left[d^{-1}\right] \times f(V)[-] \times f(P)[-] \times f(T)[-] \quad (1)$$

R_{max} describes the phenological development rate of a specific genotype under optimal environmental conditions and is equal to the reciprocal of the minimum number of days needed to complete a certain phenological phase. Accumulating daily development rates ($R = \sum r$) therefore gives information about the phenology stage of the modelled plant, with R values of -1, 0, 0.9 and 2 representing the phenology stages of sowing, emergence, heading and maturity, respectively (Wang and Engel, 1998). The vernalization, temperature and photoperiod response functions correct for suboptimal environments by multiplication of the maximum development rate with their dimensionless values in the range [0,1]. According to Wang and Engel (1998) and further elaborated by Streck et al. (2003b), the presented model equation is modified depending on the considered phenological stage as follows:

- Between plant emergence (ZS 10, according to the phenology scale of Zadoks et al. (1974)) and terminal spikelet (ZS 30): $r = r_{\max,v1} \times f(V) \times f(P) \times f(T)$
- Between terminal spikelet and anthesis (ZS 60): $r = r_{\max,v2} \times f(P) \times f(T)$
- Between anthesis and maturity (ZS 92): $r = r_{\max,r} \times f(T)$
- The time between sowing and emergence was approximated by accumulating thermal time up to 150 growing degree days, assuming a base temperature of 0 °C

The parameters $r_{max,\ v1}$, $r_{max,v2}$ and $r_{max,r}$ are genotype specific maximum development rates for each phenological phase.

The temperature response function $f(T)$ is defined as follows:

$$f(T) = \begin{cases} \dfrac{2(T - T_{\min})^{\propto}(T_{opt} - T_{\min})^{\propto} - (T - T_{\min})^{2\propto}}{(T_{opt} - T_{\min})^{2\propto}}; & if\ T_{\min} \leq T \leq T_{\max} \\ 0 & ;if\ T < T_{\min}\ \text{or}\ T > T_{\max} \end{cases} \quad (2)$$

$$\propto = \frac{\ln(2)}{\ln\left[\frac{(T_{\max} - T_{\min})}{(T_{opt} - T_{\min})}\right]} \quad (3)$$

The shape of $f(T)$ is given by the three cardinal temperatures T_{max}, T_{min} and T_{opt} representing the minimum, maximum and optimum temperature for completion of a specific phenological phase. The cardinal temperatures T_{max}, T_{min} and T_{opt} were assumed to be 30 °C, 0 °C and 19 °C for the vegetative phase from emergence until terminal spikelet, 35 °C, 4 °C and 24 °C for the vegetative phase from terminal spikelet until

heading and 35 °C, 8 °C and 24 °C for the reproductive phase from heading until maturity (Porter and Gawith, 1999; Streck et al., 2003b). T denotes the daily average temperature.

For the vernalization response function, a non-linear function proposed by (Streck et al., 2003a) was implemented:

$$f(V) = \frac{(VD)^5}{(22.5)^5 + (VD)^5} \quad (4)$$

The vernalization response function assumes full vernalization ($f(V) = 1$) after 50 effective vernalization days (VD). This threshold value agrees with the realistic range of vernalization requirements for the varieties considered in this study (Fossati, 2000). The sensitivity of simulated heading dates to differences in vernalization days within this realistic range was tested and proved to be minor (supplementary material, Fig. 1). The number of VD after sowing was calculated as $VD = \sum f_{vn}(T)$, with $f_{vn}(T)$ giving the daily vernalization rate as calculated with Eqs. (2) and (3) but the cardinal temperatures for vernalization $T_{max,vn}$, $T_{min,vn}$ and $T_{opt,vn}$ (15.7 °C, -1.3 °C and 4.9 °C, respectively) (Porter and Gawith, 1999).

The photoperiod response function of the Wang and Engel model consists of a negative exponential function:

$$f(P) = 1 - \exp[-\omega(P - P_c)] \quad (5)$$

P_c [h] therein defines a critical photoperiod below which it is assumed that no plant development can occur. ω is a measure of the cultivar specific photoperiod sensitivity [h^{-1}] and P represents the daily photoperiod depending on the day of the year (DOY) and the geographical latitude of the considered location. Regarding all response functions and maximum growth rates, a total of five genotype specific parameters ($r_{max,v1}$, $r_{max,v2}$, $r_{max,r}$, P_c, ω) need to be estimated for genotype specific model usage.

Two simplifications were conducted to increase the ratio of data points per estimated parameter:

1) Setting P_c constant to 8 h to ensure convergence of the used differential evolution algorithm (more details in section *2.2*) and avoidance of compensatory effects between ω and P_c (Eq. 5).
2) Setting $r_{max,v1} = 0.5 \times r_{max,v2}$. This simplification in the model was necessary due to the limited availability of experimental data on the phenological stage of terminal spikelet for model calibration. The assumption is based on the Wang and Engel model implementation by Streck et al. (2003b), who reported the development rate between emergence and terminal spikelet to be about 0.7 times the development rate from emergence to anthesis and by Slafer and Rawson (1995), who reported the development rate from terminal spikelet to anthesis to be about 1.4 times the development rate from emergence to anthesis.

The described model was implemented in R (R Core Team, 2019).

2.2. Experimental data, model calibration and testing

The genotype specific parameters were estimated using field data of the preliminary and official variety testing trials of the Swiss federal agricultural research institute Agroscope. The data originated from 15 field sites spread across the Swiss Plateau as indicated in Fig. 1. At each location, the tested genotypes were sown at a seeding density of 350 grains m^{-2} on a plot of 7 to 10 m^2 with three replicates. Regarding crop management, no fungicides nor growth regulators were applied. Herbicides were used only if necessary. The parcels were fertilized according to the Swiss fertilization guidelines (Richner and Sinaj, 2017). For each genotype, location and year, the date of sowing, the average heading date (ZS 57/58) and harvest date were recorded. In each year, all crops at the same location were sown and harvested on the same date. As this resulted in non-independent observations of harvest dates for the considered genotypes, we excluded this phenology stage (and the $r_{max,r}$ parameter, accordingly) from the analysis and focused only on the

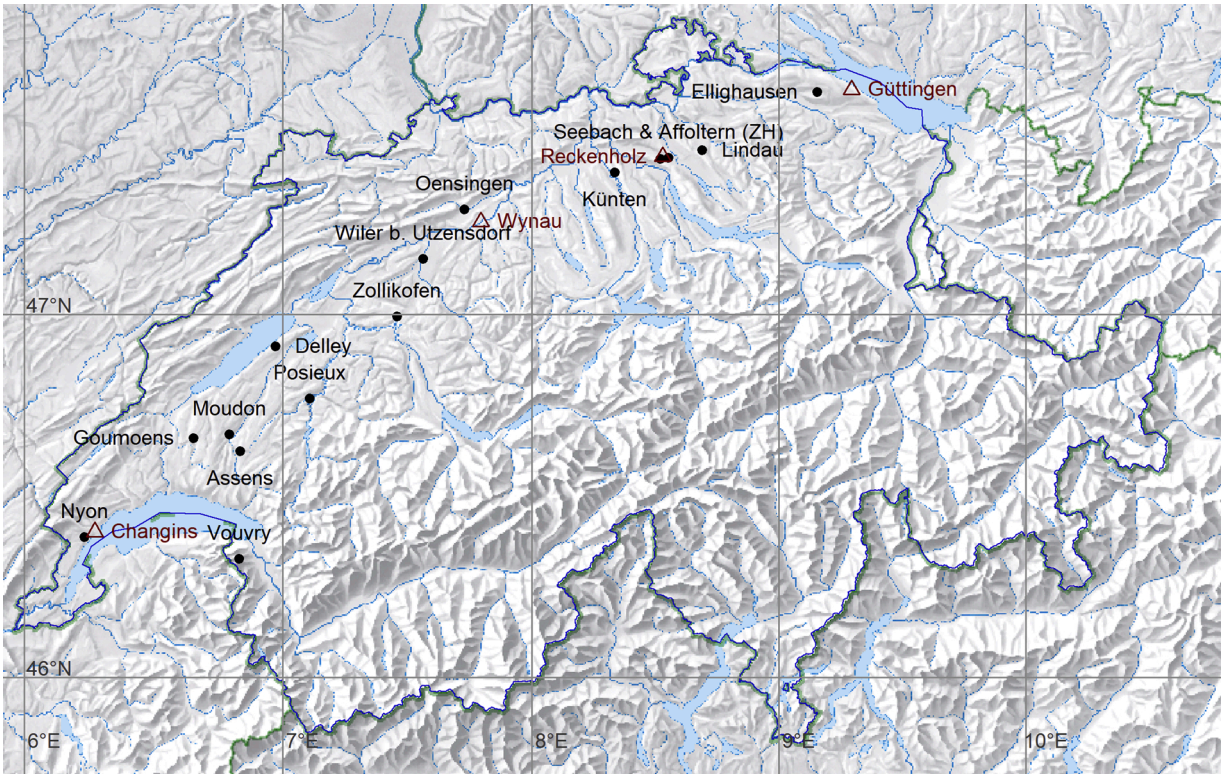

Fig. 1. Considered field sites and weather stations in the Swiss Plateau. Dots indicate field sites from which phenological data for model calibration was available. Triangles indicate locations (weather stations) for which predictions of heading dates and heat stress occurrence until 2099 were conducted. The dark blue line indicates the Swiss country border. Source: Federal Office of Topography, swisstopo (www.swisstopo.admin.ch).

Table 1
Available phenological data from Switzerland for calibration and testing of a winter wheat phenology model.

Genotype	Number of environments (year-location combinations)	Years	Locations
Arbola	37	2000–2005	Assens, Affoltern (ZH), Delley, Ellighausen, Moudon, Nyon, Oensingen, Posieux, Vouvry, Wiler b. Utzensdorf
Levis	148	2001–2018	Assens, Affoltern (ZH), Delley, Ellighausen, Goumoens, Künten, Lindau, Moudon, Nyon, Oensingen, Posieux, Seebach (ZH), Vouvry, Wiler b. Utzensdorf, Zollikofen
Arina	122	2000–2018	Assens, Affoltern (ZH), Delley, Ellighausen, Goumoens, Künten, Lindau, Moudon, Nyon, Oensingen, Posieux, Seebach (ZH), Vouvry, Wiler b. Utzensdorf, Zollikofen,
Galaxie	46	2000–2004 & 2009–2012	Assens, Affoltern (ZH), Delley, Ellighausen, Goumoens, Lindau, Moudon, Nyon, Oensingen, Posieux, Vouvry, Wiler b. Utzensdorf

phenology stage of heading.

Four genotypes are in the focus of the present study, namely Arbola, Arina, Levis and Galaxie, representative of one late, two average and one early heading winter wheat variety currently or recently cultivated in Switzerland. These four genotypes were selected to cover the range of phenological differences within the Swiss wheat production (see supplementary Fig. 2). Galaxie, Arina and Arbola have been used as earliness standards in the Swiss wheat breeding program. Data availability differed for the four selected genotypes as depicted in Table 1.

The genotypic parameters were estimated by finding a parameter set minimizing the residual sum of squares between observed and modelled heading dates (DOY when the modelled phenology index R reaches 0.9). For doing so, a differential evolution algorithm as introduced by Price et al. (2006) and implemented in the R package 'DEoptim' (Ardia et al., 2016) was used. To quantify uncertainties associated with this iterative procedure, the optimization was repeated 20 times per genotype with each time using a differing and randomly selected subset comprising 75 % of the available field data. This resulted in 20 parameter sets per genotype, which were all used in the model application explained in section *2.3*. The detailed optimization procedure consisted of the following steps: Firstly, for each experimental field the temperature data for the considered year was retrieved from the nearest weather station (www.agrometeo.ch, www.meteoswiss.admin.ch). The coordinates of the respective weather stations were used to calculate the daily photoperiod using the R package 'geosphere' (Hijmans, 2019). The median distances of the experimental fields to the nearest weather station were 1.8 km, 1.4 km, 1.4 km and 1.6 km for Arbola, Arina, Levis and Galaxie, respectively. Secondly, using the mentioned differential evolution algorithm, the parameters $r_{max,v2}$ and ω were estimated with the parameter constraints [0.03, 0.07] and [0.15, 0.4], respectively.

After each optimization run, the remaining 25 % of observational data was used for testing the model performance. The root mean square error (RMSE) between the modelled and observed heading dates of the test set was calculated as follows:

$$RMSE = \left(\frac{\sum_{1}^{n} (\widehat{y}_i - y_i)^2}{n} \right)^{1/2} \quad (6)$$

With $\widehat{y}_i$ and y_i being the modelled and observed heading DOY and n being the number of observations in the test set.

2.3. Model application

The calibrated and validated model was used to predict heading dates of the genotypes Arbola, Arina, Levis and Galaxie until the year 2099 at four locations spread across the Swiss Plateau. The considered locations were Changins (6°14′E 46°19′N, 455 m a.s.l), Wynau (7°47′E 47°15′N, 422 m a.s.l), Reckenholz (8°31′E 47°26′N, 443 m a.s.l.) and Güttingen (9°17′E 47°36′, 440 m a.s.l) and are indicated in Fig. 1.

For the required daily mean temperatures until 2099, the freely available data from the Swiss Climate Change Scenarios CH2018 was used (CH2018 Project Team, 2018). A detailed description of the scenarios can be found in CH2018 (2018). In short, the CH2018 scenarios were derived from the EURO−CORDEX ensemble of climate simulations using Regional Climate Models (RCM). As the resolution of the RCM simulations (10−25 km) is not sufficient to represent the variable topographic and climatological landscape of Switzerland, the local climate projections used in the present study were obtained by statistical downscaling of the RCM simulations. The used method, namely quantile mapping, matches the distribution of simulated and observed climate variables and applies an obtained correction to the projections of future climate. The CH2018 scenarios consider three Representative Concentration Pathways (RCPs) as defined by the Intergovernmental Panel on Climate Change (IPCC, 2013). RCPs define scenarios of future global GHG emissions, depending on the development of the global population size, economic activities, lifestyle, energy use, land use patterns and climate policy. For the present study, the scenarios RCP2.6 and RCP8.5 were considered. RCP2.6 denotes an emission scenario with a substantial reduction of global GHG emissions in order not to exceed 2 °C warming over the course of the 21st century (radiative forcing of 2.6 W m^{-2} and GHG concentration of 650 ppm CO_2 equivalents by 2100 relative to 1850–1900), whereas RCP8.5 denotes a scenario with no GHG emission reductions and an expected increase in the global mean surface temperature by 4–5 °C until the end of the century (radiative forcing of 8.5 W m^{-2} and GHG concentration 1370 ppm CO_2 equivalents by 2100 relative to 1850–1900) (CH2018, 2018). In order to capture uncertainties originating from the used climate models, temperature data from 12 model chains (RCMs coupled to a global circulation model) was used. Detailed information on the used climate model chains is

Table 2
Projected temperature changes under climate change at four Swiss sites. Average temperatures [°C] during the months March until May (MAM) and November until January (NDJ) as represented in the climate projections from 12 climate model chains for four Swiss locations, namely Changins (CGI), Güttingen (GUT), Reckenholz (REH) and Wynau (WYN) under two climate change scenarios (RCP2.6 and RCP8.5). Numbers in brackets indicate standard deviations.

Location	Historic (1982–2006)		RCP2.6 (2075–2099)		RCP8.5 (2075–2099)	
	NDJ	MAM	NDJ	MAM	NDJ	MAM
CGI	3.4 (1.1)	9.6 (1.3)	4.3 (1.3)	10.7 (1.4)	7.1 (1.3)	13.2 (1.6)
GUT	2.2 (1.3)	8.8 (1.3)	3.1 (1.5)	10.0 (1.4)	6.0 (1.4)	12.2 (1.5)
REH	2.1 (1.3)	9.0 (1.3)	3.1 (1.5)	10.0 (1.4)	6.0 (1.4)	12.3 (1.5)
WYN	1.9 (1.2)	8.5 (1.2)	2.8 (1.4)	9.5 (1.3)	5.6 (1.3)	11.7 (1.4)

shown in Table 1 of the supplementary material. Projected changes in winter and spring temperatures for the four studied sites are shown in Table 2.

For assessment of how shifts in sowing dates affect the modelled heading dates, the established model was run for five hypothetic sowing dates per year, namely October 1, 10, 20, 30 and November 10. In summary, the phenology model was run for four genotypes, four locations, five sowing dates, 20 parameter sets per genotype and using temperature data from 12 climate model chains under two RCP's.

Pre- and post-heading heat stress was estimated by calculating the following heat stress indicators:

- Heat days around heading (HD_H): the number of days with a daily maximum temperature above 30 °C in a period from -5 to +10 days around the predicted heading date.
- Average maximum temperature around heading (AMT_H): the average daily maximum temperature during the same period from -5 to +10 days around heading. This indicator depicts heat stress intensity.
- Heat days during grain filling (HD_{GF}): the number of days with a daily maximum temperature above 30 °C in a time window from +11 to +30 days after heading.
- Average maximum temperature during grain filling (AMT_{GF}): the average daily maximum temperature during the same period from +11 to +30 days after heading.

The indicators were defined based on reviews on temperature effects on wheat by Porter and Gawith (1999) and Barlow et al. (2015). In the definition of the heat stress indicators, it is assumed that 30 days after heading, all varieties have completed the phenological development sensitive to heat stress. Doing so, it was assumed that differences in the exact duration of grain filling between varieties and heat stress during the latest stages of grain filling (>30 days after heading) are of minor importance. This is supported by the observation of heat stress effects predominantly occurring between heading and early grain filling (Barlow et al., 2015), which is covered by the considered time period of the indicators. Finally, in order to compare heat stress occurrence to the case without considering phenological dynamics, heat stress indicators were additionally calculated for a hypothetic genotype with a fixed heading date on DOY 155 (beginning of June).

2.4. Analysis of projected heading dates and heat stress indicators

To disentangle influences of single factors (i.e. location, genotype, sowing date, genotypic model parametrization, climate model chain and RCP scenario) on the variation of projected heading dates and heat stress indicators, an ANOVA-based partitioning of total variation was applied (Yip et al., 2011). Thereby, the percentage of variation attributed to one factor equals the ratio of the factor's sum of squares divided by the total sum of squares. In the conducted decomposition of total variation, we considered the effects of single factors as well as two-way-interaction effects. Not explicitly considered higher order interactions are in the following included in the so-called "residual" variation. Year-to-year climate variability was averaged out by analysing 25-year mean values (starting with the period 1982−2006) of heading dates and heat stress indicators of each location, genotype, sowing date, parameter set, climate model chain and RCP scenario combination.

The statistical analysis was done using R (R Core Team, 2019). Graphical output was obtained using the R package ggplot2 (Wickham, 2016).

3. Results

3.1. Model performance

The average RMSE between observed and modelled heading dates across all genotypes was 3.6 days with a standard error of 0.7 days. In tendency, the variation in RMSE observed in the 20 model testing runs was smaller for genotypes with a larger set of experimental data available for model calibration and testing (Table 3). A plot of the measured and modelled heading dates for one of the 20 calibration and testing runs per genotype is presented in supplementary Fig. 3. The ranking of the estimated development rates $r_{max,v2}$ is in accordance with field observations of Arbola as the latest (lowest development rate) and Galaxie as the earliest genotype among the considered.

Table 3
Phenology model calibration results. Average root mean square error (RMSE) between modelled and observed heading dates per genotype, estimated genotype specific photosensitivity (ω) and maximum development rate between the phenology stages of terminal spikelet and anthesis ($r_{max,v2}$). Parameter estimation and model testing was repeated 20 times per genotype with always a randomly selected subset of 75 % of the available field data for parameter estimation and 25 % for model testing. Parameter estimation was done using a differential evolution algorithm minimizing the residual sum of squares between observed and modelled heading dates. Numbers in brackets give the standard deviation.

Genotype	$RMSE_{calibration}$ [days]	$RMSE_{testing}$ [days]	ω [h^{-1}]	$r_{max,v2}$ [d^{-1}]
Arbola	3.2 (0.2)	3.9 (0.7)	0.17 (0.02)	0.039 (0.002)
Arina	3.7 (0.2)	3.7 (0.5)	0.18 (0.03)	0.041 (0.003)
Levis	3.9 (0.1)	3.9 (0.4)	0.16 (0.01)	0.045 (0.002)
Galaxie	3.02 (0.2)	3.0 (0.7)	0.16 (0.02)	0.048 (0.002)

3.2. Shift in heading dates

A steady advancement of the 25-year median heading date across all genotypes, locations, RCP's, sowing dates and climate model chains was modelled (Fig. 2A). RCP was the most influential factor regarding the timing of winter wheat heading throughout the second half of the 21st century. Accordingly, RCP explained 57 % of the total modelled variation in average heading dates for the period 2075−2099 (last 25-year sliding window considered). During the respective period, the average heading date was DOY 148 and DOY 135 for RCP2.6 and RCP8.5, respectively. Compared to the reference period 1982−2006 (average heading date DOY 154), this equals an advancement of winter wheat heading dates by 6 and 19 days, respectively. Applying a linear regression to the modelled heading dates over time (2020–2099) revealed an average advancement rate of 2.6 and 0.2 days per decade with RCP8.5 and RCP2.6, respectively. The factors genotype, location and sowing date contributed 12 %, 11 % and 2% to total variability in average heading dates for the sliding window of 2075−2099. For the same period, considerable variation in projected heading dates could be attributed to differences in the climate models (12 % of total variation). Uncertainties in the genotypic parametrization were assessed to be of little importance (<1% of total variation).

Genotypic differences in heading dates as observed under current climatic conditions were modelled to remain important under both RCP scenarios (Fig. 2, B). Additionally, estimated heading dates followed a strong geographical pattern with earliest heading dates in Changins and latest heading dates in Wynau.

A strong negative correlation between heading dates and average temperatures during the months March until May was predicted (Fig. 3A). With RCP8.5, heading dates were modelled to advance by 5.6 days per 1 °C increase in the average temperature during the respective months. Accordingly, the mentioned geographical pattern in heading dates followed the inverse ranking of average spring temperatures at the four studied sites (Table 2). Additionally, with ongoing climate change, the model predicted vernalization to be completed earlier in the year

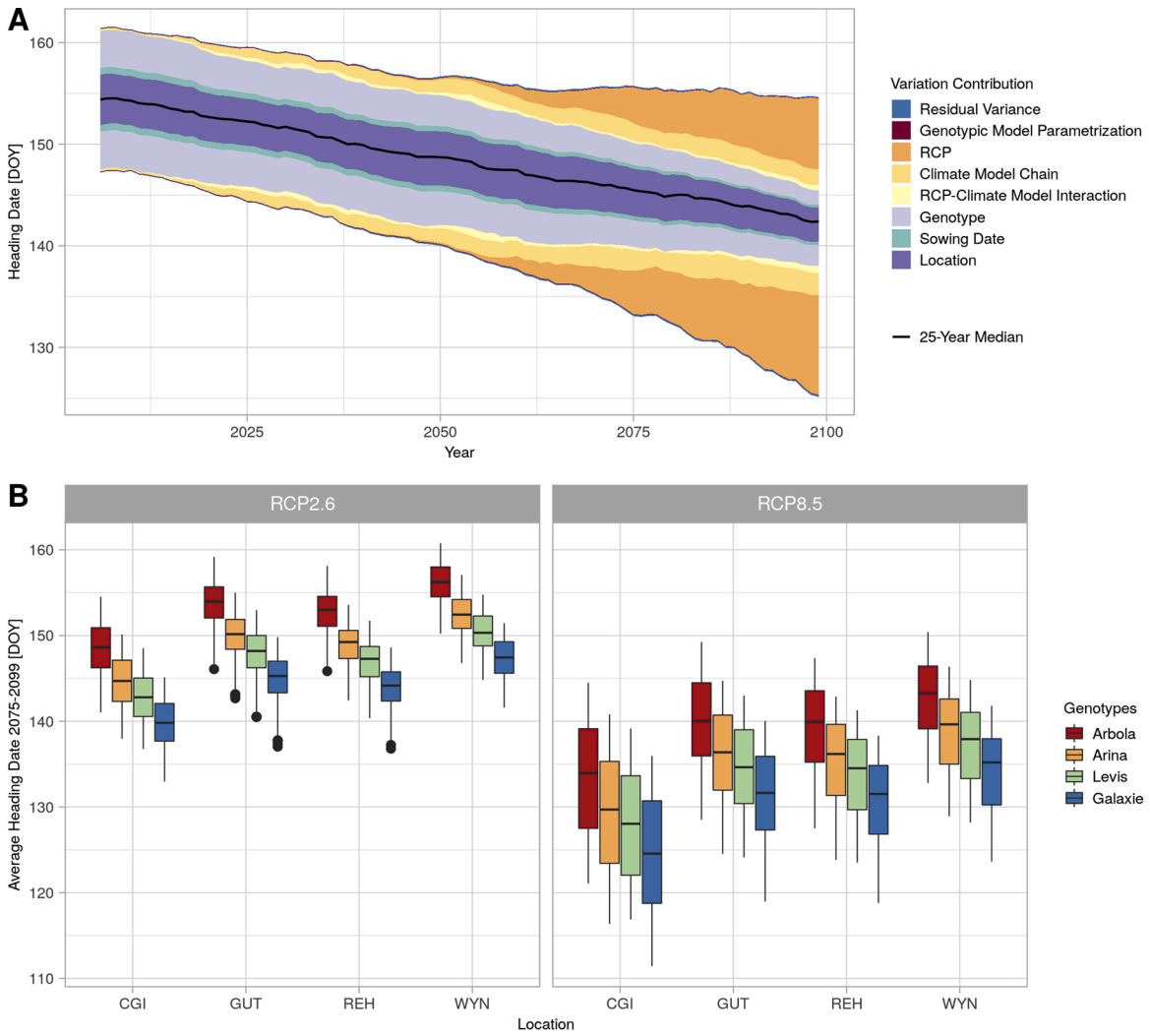

Fig. 2. Projected shift in winter wheat heading dates in Switzerland. A) Partitioning of variation of 25-year average heading date predictions for four Swiss winter wheat genotypes (Arbola, Arina, Levis, Galaxie) under two climate change scenarios (RCP2.6 and RCP8.5), using temperature data from 12 climate model chains, at four locations spread across the Swiss Plateau, for five sowing dates (between Oct. 1 and Nov. 10) and 20 model parametrizations per genotype. The black line indicates the median of the respective 25-year sliding window (starting with 1982-2006). The width of the colored band equals the range between the 5th and 95th percentile of the predicted heading dates in the respective sliding window. Each color indicates the percentage of total variation attributable to the mentioned factors. B) Average heading date predictions for the years 2075-2099 for each combination of the mentioned factors.

(Fig. 3B). Yet the effect of increasing spring temperatures was of greater importance regarding the modelled heading dates than the advancement of the day of complete vernalization (adjusted R^2 of 0.83 compared to 0.004).

3.3. Heat stress occurrence

Heat stress during the winter wheat heading and grain filling period was modelled to increase during the second half of the 21st century (Fig. 4). Thereby, a considerable increase was only predicted for RCP8.5. With RCP2.6, heat stress levels remained fairly stable throughout the 21st century. Average HD_H were modelled to increase from 0.3 days in 1982–2006 (average of both RCPs) to 0.4 and 0.9 days in 2075–2099 under RCP2.6 and RCP8.5, respectively (Fig. 4A). Average HD_{GF} increased from 1.2 days in 1982–2006 (average for both RCPs) to 1.7 and 2.8 days in 2075–2099 under RCP2.6 and RCP8.5, respectively (Fig. 4B). The AMT_H was observed to decrease by 0.2 °C under RCP2.6 and to increase by 0.3 °C under RCP8.5 (Fig. 4C). Regarding the AMT_{GF} an increase of 0.4 °C and 1.0 °C was modelled for RCP2.6 and RCP8.5, respectively (Fig. 4D). A substantially higher level of heat stress was modelled for a hypothetic genotype with a static heading date on DOY 155. For the latter, under RCP8.5, HD_H were modelled to increase from an average of 0.3 days in 1982–2006 to 2.5 days in 2075–2099. HD_{GF} increased from an average of 1.3 days in 1982–2006 to 6.2 days in 2075–2099. Additionally, an increase in the average maximum temperature of 2.9 °C for the heading period and 3.9 °C for the grain filling phase was estimated (Fig. 4). The difference in heat stress between the genotype with a static heading date and the average heat stress days modelled for the other genotypes (difference in the sum of HD_H and HD_{GF} of 5.1 heat days under RCP8.5 for 2075–2099) represents a heat stress escape mechanism due to a general advancement of heading dates under climate change. This effect was also modelled to occur under the RCP2.6 scenario, even though on a smaller scale (data not shown).

Partitioning of the total variation in the average HD_H for the period 2075–2099 revealed that locational differences were important with both RCP's (Table 4). Genotypic effects ranked behind the RCP effect as well as climate model and climate model-RCP interaction uncertainties.

The locational and genotypic pattern of heat stress was largely the same as for the predicted heading dates. Thereby, later heading dates resulted in a higher number of heat stress days (Fig. 5). An exception was the location Reckenholz which showed a tendency of increased heat stress despite similar heading dates as in Güttingen. The number of heat

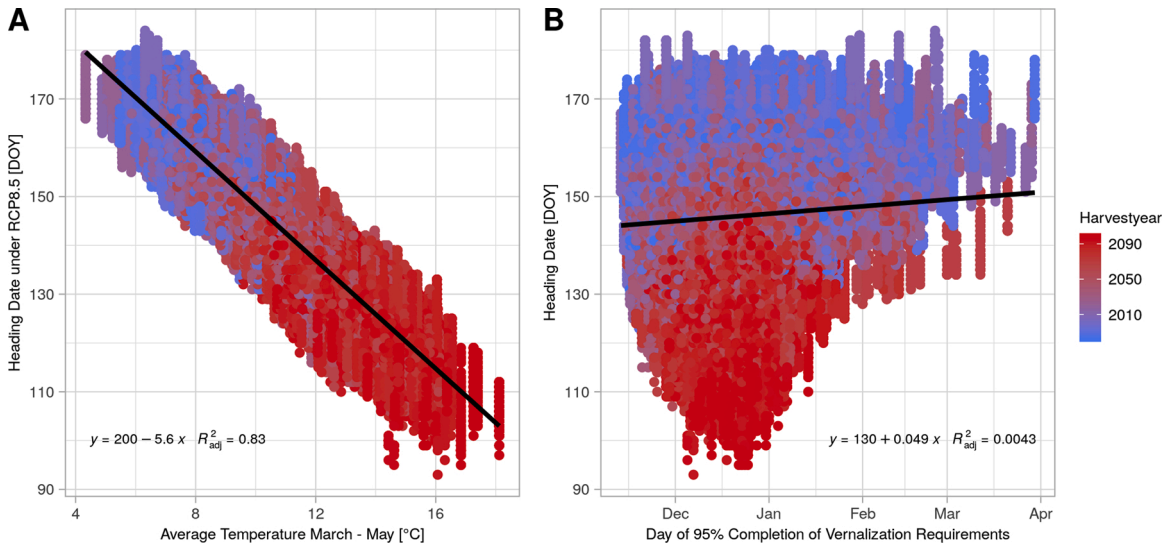

Fig. 3. Effect of spring temperatures and vernalization on heading dates. Linear regression between modelled heading dates under the RCP8.5 climate change scenario until the year 2099 and A) average spring temperatures and B) day of the year (DOY) of 95 % complete vernalization. Heading dates were modelled for four genotypes (Arbola, Arina, Levis Galaxie), at four Swiss locations (Changins, Güttingen, Reckenholz, Wynau), five sowing dates (between Oct. 1 and Nov. 10), 12 climate model chains and 20 model parametrizations per genotype.

stress days predicted for the earliest genotype Galaxie under RCP8.5 was in the range as modelled for late genotypes under the RCP2.6 scenario and for some locations even as under the reference climate in 1982–2006. HD_{GF} as well as AMT_H and AMT_{GF} followed the same pattern as observed for HD_H (supplementary material, Fig. 5). Considering the average sum of HD_H and HD_{GF}, the difference in heat stress days between the latest genotype Arbola and the earliest genotype Galaxie amounted to 1.0 and 1.6 heat days under the RCP2.6 and RCP8.5 scenario, respectively.

4. Discussion

4.1. Phenology shifts with future climate change

Climate change without climate mitigation measures was modelled to have a strong effect on the heading dates of contemporary winter wheat varieties in Switzerland. With RCP8.5, heading dates were predicted to advance by approximately 2.6 days per decade compared to 0.2 with RCP2.6. This shift is in the range of other modelling studies for Europe, which generally agree on an advancement of anthesis and heading dates by one to two weeks until the mid-21st century assuming a high GHG emission scenario (Gouache et al., 2012; Olesen et al., 2012; Semenov, 2009; Trnka et al., 2014). Further, the modelled advancement rate is similar to historical heading date trends as observed in Germany (2.1 days decade $^{-1}$; 1951–2004), the US great plains (1.5 days decade^{-1}; 1948–2004), the Loess Plateau in China (3.7 days decade^{-1}; 1981–2009) (Estrella et al., 2007; He et al., 2015; Hu et al., 2005). The same trend is also visible in the phenology data that was used for model calibration in the present study (supplementary material, figure 6). In all mentioned studies considering historical phenology data, a strong negative correlation of heading dates and spring temperatures was revealed. This is supported by our findings, with a modelled advancement of heading dates by 5.6 days per 1 °C increase in the average temperature from March until May under RCP8.5. Moreover, we also identified a tendency of an earlier fulfilment of vernalization requirements under climate change. This is a result of increasing winter temperatures towards the assumed optimum vernalization temperature of 4.9 °C. Such an effect is only to be expected in regions currently revealing winter temperatures below the vernalization optimum (e.g., Switzerland or other regions in Northern Europe) (Harrison et al., 2000). For warmer climates (e.g., Australia, Southern Spain), increased winter temperatures were predicted to substantially delay winter wheat development due to incomplete vernalization (Guereña et al., 2001; Wang et al., 2015). Nevertheless, increased average spring temperatures had a considerably stronger influence on winter wheat heading dates than a shortening of the vernalization period.

4.2. Heat stress exposure with future climate change

Results derived with RCP2.6 suggest that with climate mitigation, heat stress exposure of winter wheat would remain largely at its current level. Under the RCP8.5 scenario, heat stress was modelled to increase for all genotypes and locations over the second half of the 21st century. This is in accordance with other modelling studies for other regions of Europe (Gouache et al., 2012; Semenov, 2009; Strer et al., 2018; Trnka et al., 2014). Summing up average HD_H and HD_{GF} under RCP8.5, an increase of 2.1 heat days was predicted by the end of the 21st century. Average maximum temperatures during the heading and post-heading phase increased by 0.3 °C and 1.0 °C, respectively. However, modelled heat stress indicators increased at a considerably larger rate assuming a static heading date in early June (increase in heat stress days of 7.1 days). This substantial difference indicates that Swiss wheat production can considerably benefit from the escape of heat stress periods by an overall advanced winter wheat phenology. Thereby, the phenological phases of wheat heading and grain filling are shifted to periods with lower temperatures. This is in line with observations on historical phenological dynamics and the abundance of heat stress periods in Germany during the period 1951–2009 (Rezaei et al., 2015). Despite this effect, heat stress exposure of winter wheat is projected to increase steadily in the second half of the century (~from 2060 onwards). This suggests that there will be an increasing need to account for heat stress in future wheat breeding in Switzerland.

The genotypic contribution to total variation in heat stress days was predicted to be smaller than location effects. This implies that the considered spectrum of phenological differences between varieties is not sufficient to fully compensate regional climate variation across the Swiss Central Plateau. Heat stress exposure is lowest at the warmest location (CGI = Changins) with the fastest phenological development, and largest at the coolest site (WYN = Wynau) as shown in Fig. 5. The earliest variety (Galaxie) still shows a higher heat exposure at Wynau than the latest variety (Arbola) at Changins. This is true under current and even more so, under future climate conditions, which suggests an

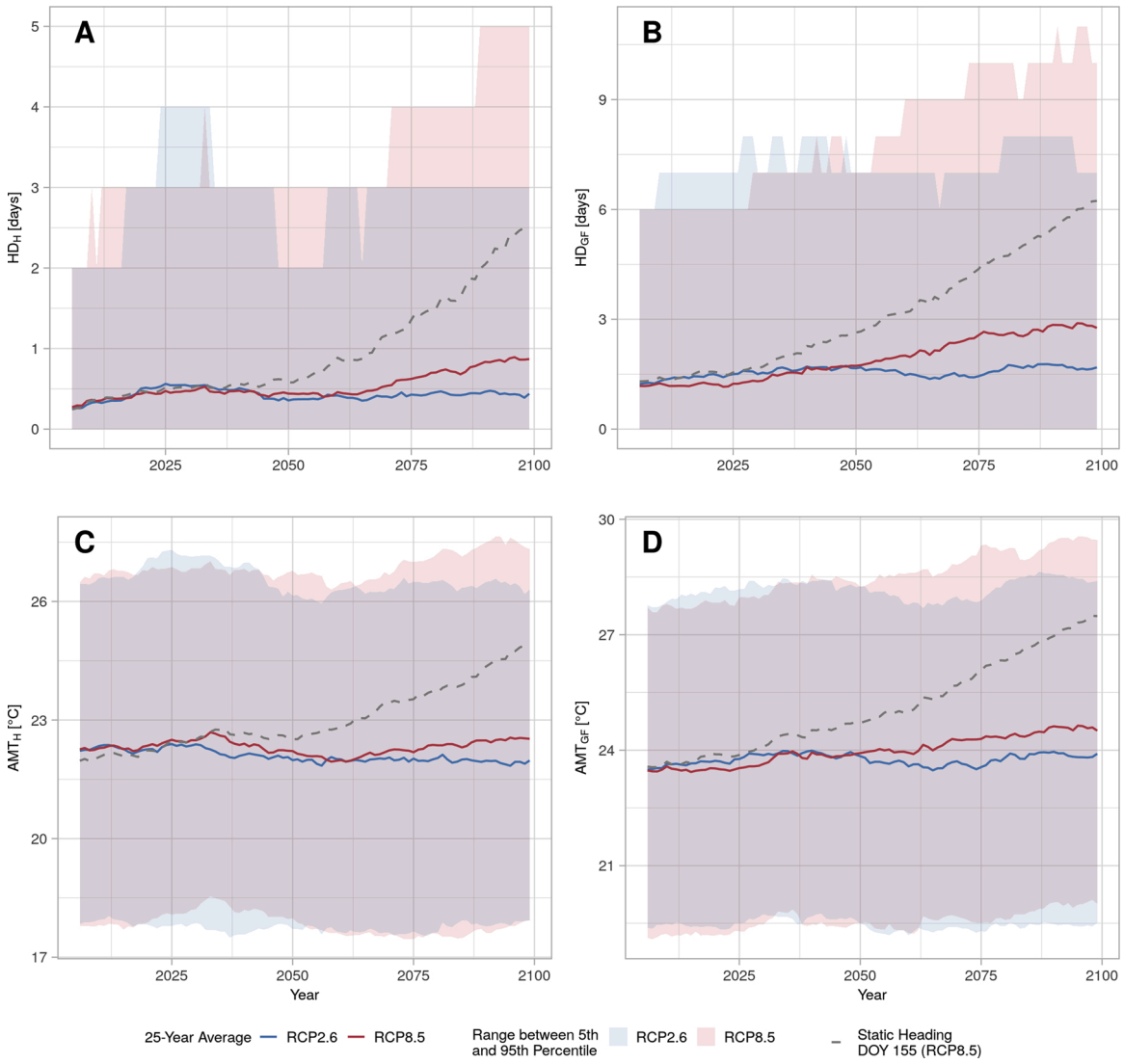

Fig. 4. Heat stress occurrence under climate change. Colored lines indicate the ensemble mean as a 25-year sliding average (starting with 1982-2006), colored bands indicate the range between the 5th and 95th percentile of heat stress indicators modelled for four Swiss winter wheat genotypes (Arbola, Arina, Levis and Galaxie), under two climate change scenarios (RCP2.6 and RCP8.5), using temperature data from 12 climate model chains, at four locations spread across the Swiss Plateau, for five sowing dates (between Oct. 1 and Nov. 10) and 20 model parametrizations per genotype. Dashed grey lines indicate 25-year averages of heat stress indicators modelled for a hypothetic genotype with a static heading date in early June (day of the year 155) under the climate change scenario RCP8.5 (more details including 5th and 95th percentiles and values under RCP2.6 in Fig. 4 of the supplementary material). A) heat days around heading (HD_H): number of days with maximum temperatures above 30 °C in a period from -5 to +10 days around the modelled heading dates, B) heat days during grain filling (HD_{GF}): number of days with maximum temperatures above 30 °C in period from +11 to +30 days after the modelled heading dates, C) average maximum temperature during the respective heading period (AMT_H), D) average maximum temperature during the respective grain filling period (AMT_{GF}).

increasing need for further breeding and accurate cultivars selection to improve adaptations to regional climatic differences within Switzerland. Interestingly, when comparing the locations Reckenholz (REH) and Güttingen (GUT), a stronger tendency of increased heat stress was identified for Reckenholz compared to for Güttingen, despite similar heading dates at both sites. This can be explained by a smaller seasonal temperature variability at Güttigen in proximity to Lake Constance.

Our study results may suggest that breeding efforts to reduce heat stress could be directed at phenological earliness for heat escape (see also Gouache et al., 2012; Mondal et al., 2016; Trnka et al., 2014). However, such a strategy could have several drawbacks. Firstly, increased earliness may imply an increased exposure of sensitive growth stages to late frost and increased radiation limitations during meiosis (e.g. Demotes-Mainard et al., 1995). Secondly, earliness could potentially be an effective strategy for the preceding and shorter phase of phenological development between heading and flowering but might not be sufficient for the later and longer lasting grain filling period, during which also under current climatic conditions heat events are more common. Even though the heading and anthesis period is considered the most susceptible to heat events, already mild heat waves during grain filling (i.e. 10–20 days after anthesis) caused yield reductions of 10 % and more under field conditions (Elía et al., 2018), pointing towards additional adaption strategies needed during this stage of the development. Finally, earliness often comes at the cost of reduced yield potentials as there is less time for photosynthesis and biomass accumulation (Shpiler and Blum, 1986). Shortened growing periods are considered a main driver of reduced wheat grain yields under climate change (Asseng et al., 2015; Trnka et al. 2014) and are likely a reason for plateaued trends of wheat yields in Europe (Brisson et al., 2010), including Switzerland (Herrera et al., 2019). In line with that, ideotype studies had previously identified the breeding of cultivars with prolonged grain filling periods as key to improve wheat yield potentials in Europe

Table 4
Factor contribution to modelled variation in heat days. Partitioning of total modelled variation in heat stress days around heading (HD_H) into the factors genotype (Arbola, Arina, Levis, Sertori), location (Changins, Güttingen, Reckenholz, Wynau), sowing date (5 dates between Oct. 1 and Nov. 10), RCP scenario (RCP2.6 and RCP8.5), climate model chain (n = 12), genotype-specific model parametrization (20 parameter estimation runs) according to their contribution to the total observed sum of squares.

Factor	Contribution to total variation in average HD_H 2075−2099 [%]
Location	26
Model	21
RCP	17
RCP:Model-Interaction	11
Genotype	7
Model:Location-Interaction	5
Model:Genotype-Interaction	2
RCP:Location-Interaction	1
Sowingday	1
Residual	~9

(Semenov et al., 2014; Senepati and Semenov, 2020). Results of our study suggest that a strategy of phenological earliness should be complemented with efforts to improve heat tolerance traits (see also Gouache et al., 2012; Stratonovitch and Semenov, 2015). Moreover, it is likely that such varieties should also have increased tolerances to other extreme weather events potentially occurring at increased frequency during summer months such as strong precipitation or drought (Rummukainen, 2012).

It is thus a key challenge of future wheat breeding programs to find an appropriate balance between phenological adaptations and an increased tolerance to abiotic stresses such as heat. The breeding for heat tolerant genotypes is challenging due to the complexity of heat tolerance traits as well as the limited availability of fast and accurate phenotyping strategies to screen and select for such (Cossani and Reynolds, 2012; Farooq et al., 2011). Yet, a considerable genetic variation regarding tolerance to heat as well as to drought and heavy precipitation events was assessed among European wheat genotypes (Mäkinen et al., 2018). Introducing these traits into high-yielding, locally adapted genotypes represents a major challenge to wheat breeding programs. Particularly the adaptation of cultivars to extreme events will be difficult to address in a routine breeding program. Yet the predicted increase in the frequency of intense and/or long heat events in Europe (Schär et al., 2004; Seneviratne et al., 2006) will force breeders to seek for adequate breeding strategies.

4.3. Model uncertainties

The performance of the fitted variety-specific phenology models was very good (see Table 3). The presented results depict clear trends regarding future winter wheat phenology and heat stress occurrence in Switzerland. Yet, the projections are subject to several sources of uncertainty. Two main sources are climate model uncertainties and structural uncertainties in the used phenology model. In the present study, climate model uncertainties were quantified by using temperature data from 12 climate model chains. As in other modelling studies of similar character (e.g., Gouache et al., 2012; Olesen et al., 2012; Trnka et al., 2014; Wang et al., 2015), differences between climate models added considerably to total variation in modelled heading dates and heat stress indicators. A detailed discussion on the causes and implications of the uncertainties associated with the climate change projections for Switzerland can be found in CH2018 (2018). Uncertainties in the wheat phenology model applied in this study have several reasons. Firstly, the model only considers a limited number of environmental drivers as influential on crop phenology. These environmental drivers are daily mean temperatures, temperature-driven vernalization and photoperiod, as it is the case in most wheat phenology models (Wu et al., 2017). Under climate change also water availability and atmospheric CO_2 concentrations could potentially affect crop phenology (Slafer and Rawson, 1994). Yet, full understanding and accurate quantification of these effects on wheat remains a challenge to be overcome (McMaster and Wilhelm, 2003; Saebo and Mortensen, 1996; Springer and Ward, 2007). Secondly, several broad assumptions were taken on how the studied genotypes react to the mentioned environmental drivers. For instance, it is assumed that all genotypes reveal the same cardinal temperatures and vernalization requirements. Such simplifications limit the ability to detect detailed genotype, location and climate interaction effects. However, in the context of limited availability of data for model calibration, these assumptions were evaluated as robust for a wide range of geographical regions and genotypes (Streck et al., 2003a, b; Wang and Engel, 1998; Xue et al., 2004). Looking ahead, new, non-invasive

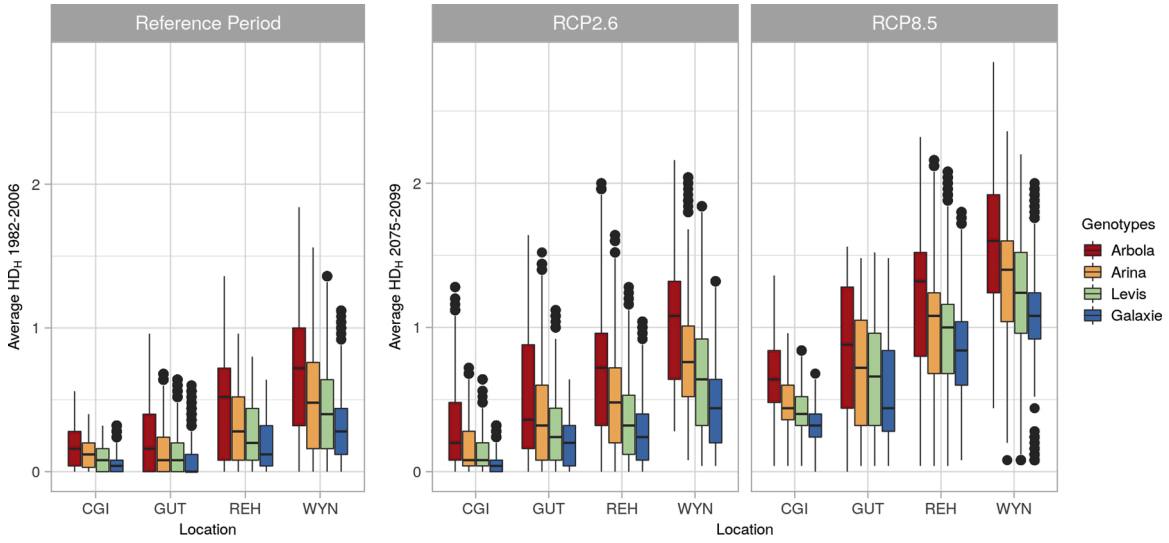

Fig. 5. Projected heat stress occurrence around winter wheat heading. Average heat days ($T_{max} \geq 30$ °C) around winter wheat heading (-5 to +10 days) (HD_H) for the reference period 1982-2006 (left) and the period 2075-2099 with both RCP2.6- and RCP8.5-projections (right) modelled for four Swiss genotypes (Arbola, Arina, Levis, Galaxie) at four locations across the Swiss Plateau, namely Changins (CGI), Güttingen (GUT), Reckenholz (REH) and Wynau (WYN). Each boxplot comprises model results for 12 climate model chains, 20 different model parametrizations per genotype, and 5 hypothetic sowing dates (between Oct. 1 and Nov. 10).

high-throughput field phenotyping methods will deliver, genotype-specific information of the timing of critical phenological stages for model calibration (Hund et al., 2019). These include the beginning of stem elongation (Kronenberg et al., 2017) or physiological maturity (Anderegg et al., 2019). Increased knowledge about the genetic and environmental drivers of these stages and the ability to efficiently screen and select for phenology related traits could thus enable an increase in yield potentials of future genotypes by breeding for an advantageous phenological development while simultaneously escaping abiotic stress periods.

Another uncertainty to be considered is the assumed fixed length of the heat stress sensitive period of phenological development (30 days from heading), applied in the calculation of heat stress indicators. It is assumed that with the chosen period length, the largest part of the heat sensitive period is covered for the considered varieties under current climatic conditions. Yet, it can be expected that under future, warmer climatic conditions, the grain filling period of a specific variety is shortened. With a fixed threshold of 30 days, heat stress days could thus be overestimated for warmer climates and shorter grain filling periods. However, a fixed threshold was applied as no phenological data of maturity (end of grain filling) was available for the considered varieties, preventing an estimation of the grain filling period under future climatic conditions.

Finally, the uncertainty related to the iterative estimation of the genotypic model parameters by a differential evolution algorithm and using 20 times a differing subset of the available field data was assessed to be negligible. Considering the satisfactory model performance, we thus consider the chosen parameter estimation procedure as robust.

5. Conclusion

In this study, it was found that without climate mitigation (RCP8.5), heat stress exposure of winter wheat during heading and early grain filling is likely to increase in Switzerland during the second half of the 21st century despite mechanisms of phenological heat escape. The adoption of earlier winter wheat genotypes would likely enable further escape from heat exposure in Switzerland. This strategy, however, may imply increased risks of late frost and low radiation during meiosis. Also, it may contradict with efforts to extend grain filling periods in order to increase yield potentials.

Considering this, further studies are needed to account for possible trade-offs with regard to frost exposure, radiation limitations and reductions in production potentials with shortened growing cycles. In view of an expected increase in inter-annual climate variability and extreme years in Europe, strategies of phenological cultivar diversification and improved heat tolerance traits might be particularly promising. Future work should also account for impacts of other extreme weather events, such as heavy precipitation, drought as well as their interactions.

CRediT authorship contribution statement

Julian Rogger: Conceptualization, Methodology, Software, Formal analysis, Visualization, Writing – original draft. **Andreas Hund:** Writing – review & editing, Resources. **Dario Fossati:** Writing – review & editing, Resources. **Annelie Holzkämper:** Conceptualization, Methodology, Writing – review & editing, Project administration.

Declaration of Competing Interest

The authors declare that they have no known competing financial interests or personal relationships that could have appeared to influence the work reported in this paper.

Appendix A. Supplementary data

Supplementary material related to this article can be found, in the online version, at doi:https://doi.org/10.1016/j.eja.2021.126394.

References

Anderegg, J., Yu, K., Aasen, H., Walter, A., Liebisch, F., Hund, A., 2019. Spectral vegetation indices to track senescence dynamics in diverse wheat germplasm. Front. Plant Sci. 10, 1749. https://doi.org/10.3389/fpls.2019.01749.

Ardia, D., Mullen, K.M., Peterson, B.G., Ulrich, J., 2016. 'DEoptim': differential Evolution in 'R'. Version 2, 2–4.

Aslam, M.A., Ahmed, M., Stöckle, C.O., Higgins, S.S., Hassan, Fu, Hayat, R., 2017. Can growing degree days and photoperiod predict spring wheat phenology? Front. Environ. Sci. 5, 1–10. https://doi.org/10.3389/fenvs.2017.00057.

Asseng, S., Ewert, F., Martre, P., Rötter, R.P., Lobell, D.B., Cammarano, D., Kimball, B.A., Ottman, M.J., Wall, G.W., White, J.W., Reynolds, M.P., Alderman, P.D., Prasad, P.V. V., Aggarwal, P.K., Anothai, J., Basso, B., Biernath, C., Challinor, A.J., De Sanctis, G., Doltra, J., Fereres, E., Garcia-Vila, M., Gayler, S., Hoogenboom, G., Hunt, L.A., Izaurralde, R.C., Jabloun, M., Jones, C.D., Kersebaum, K.C., Koehler, A.K., Müller, C., Naresh Kumar, S., Nendel, C., O'Leary, G., Olesen, J.E., Palosuo, T., Priesack, E., Eyshi Rezaei, E., Ruane, A.C., Semenov, M.A., Shcherbak, I., Stöckle, C., Stratonovitch, P., Streck, T., Supit, I., Tao, F., Thorburn, P.J., Waha, K., Wang, E., Wallach, D., Wolf, J., Zhao, Z., Zhu, Y., 2015. Rising temperatures reduce global wheat production. Nat. Clim. Change. 5, 143–147. https://doi.org/10.1038/nclimate2470.

Barlow, K.M., Christy, B.P., O'Leary, G.J., Riffkin, P.A., Nuttall, J.G., 2015. Simulating the impact of extreme heat and frost events on wheat crop production: a review. Field Crops Res. 171, 109–119. https://doi.org/10.1016/j.fcr.2014.11.010.

Brisson, N., Gate, P., Gouache, D., Charmet, G., Oury, F.-X., Huard, F., 2010. Why are wheat yields stagnating in Europe? A comprehensive data analysis for France. Field Crops Res. 119, 201–212. https://doi.org/10.1016/j.fcr.2010.07.012.

CH2018, 2018. CH2018 - Climate Scenarios for Switzerland, Technical Report, National Centre for Climate Services, Zürich. ISBN: 978-3-9525031-4-0, pp. 271.

CH2018 Project Team, 2018. CH2018 - Climate Scenarios for Switzerland. National Centre for Climate Services. https://doi.org/10.18751/Climate/Scenarios/CH2018/1.0.

Cossani, C.M., Reynolds, M.P., 2012. Physiological traits for improving heat tolerance in wheat. Plant Physiol. 160, 1710–1718. https://doi.org/10.1104/pp.112.207753.

Demotes-Mainard, S., Doussinault, G., Meynard, Jm., 1995. Effects of low radiation and low temperature at meiosis on pollen viability and grain set in wheat. Agronomie 15, 357–365.

Elía, M., Slafer, G.A., Savin, R., 2018. Yield and grain weight responses to post-anthesis increases in maximum temperature under field grown wheat as modified by nitrogen supply. Field Crops Res. 221, 228–237. https://doi.org/10.1016/j.fcr.2018.02.030.

Entz, M.H., Fowler, D.B., 1988. Critical stress periods affecting productivity of no-till winter wheat in western Canada. Agron. J. 80, 987–992. https://doi.org/10.2134/agronj1988.00021962008000060030x.

Estrella, N., Sparks, T.H., Menzel, A., 2007. Trends and temperature response in the phenology of crops in Germany. Glob. Change Biol. 13, 1737–1747. https://doi.org/10.1111/j.1365-2486.2007.01374.x.

Farooq, M., Bramley, H., Palta, J.A., Siddique, K.H.M., 2011. Heat stress in wheat during reproductive and grain-filling phases. Crit. Rev. Plant Sci. 30, 491–507. https://doi.org/10.1080/07352689.2011.615687.

Fossati, D., 2000. Alternativité, précocité et resistance au froid de quelques variétés de céréales. Rev. Suisse Agric. 32, 113–116.

Gouache, D., Le Bris, X., Bogard, M., Deudon, O., Pagé, C., Gate, P., 2012. Evaluating agronomic adaptation options to increasing heat stress under climate change during wheat grain filling in France. Eur. J. Agron. 39, 62–70. https://doi.org/10.1016/j.eja.2012.01.009.

Guereña, A., Ruiz-Ramos, M., Dìaz-Ambrona, C.H., José, R.C., Mînguez, M.I., 2001. Assessment of climate change and agriculture in Spain using climate models. Agron. J. 93, 237–249. https://doi.org/10.2134/agronj2001.931237x.

Harrison, P.A., Porter, J.R., Downing, T.E., 2000. Scaling-up the AFRCWHEAT2 model to assess phenological development for wheat in Europe. Agric. For. Meteorol. 101, 167–186. https://doi.org/10.1016/S0168-1923(99)00164-1.

He, L., Asseng, S., Zhao, G., Wu, D., Yang, X., Zhuang, W., Jin, N., Yu, Q., 2015. Impacts of recent climate warming, cultivar changes, and crop management on winter wheat phenology across the Loess Plateau of China. Agric. For. Meteorol. 200, 135–143. https://doi.org/10.1016/j.agrformet.2014.09.011.

Herrera, J.M., Levy Haner, L., Mascher, F., Hiltbrunner, J., Fossati, D., Brabant, C., Charles, R., Pellet, D., 2019. Lessons from 20 years of studies of wheat genotypes in multiple environments and under contrasting production systems. Front. Plant Sci. 10, 1745. https://doi.org/10.3389/fpls.2019.01745.

Hijmans, R.J., 2019. Geosphere: Spherical Trigonometry. R Package Version 1, pp. 5–10.

Holzkämper, A., Fossati, D., Hiltbrunner, J., Fuhrer, J., 2014. Spatial and temporal trends in agro-climatic limitations to production potentials for grain maize and winter wheat in Switzerland. Reg. Environ. Change 15, 109–122. https://doi.org/10.1007/s10113-014-0627-7.

Hu, Q., Weiss, A., Feng, S., Baenziger, P.S., 2005. Earlier winter wheat heading dates and warmer spring in the U.S. Great Plains. Agric. For. Meteorol. 135, 284–290. https://doi.org/10.1016/j.agrformet.2006.01.001.

Hund, A., Kronenberg, L., Anderegg, J., Yu, K., Walter, A., 2019. Non-invasive Field Phenotyping of Cereal Development, Advances in Breeding Techniques for Cereal

Crops. Burleigh Dodds Series in Agricultural Science. Buleigh Dodds Science Publishing, Cambridge UK, pp. 44.
IPCC, 2013. In: Stocker, T.F., Qin, D., Plattner, G.-K., Tignor, M., Allen, S.K., Boschung, J., Nauels, A., Xia, Y., Bex, V., Midgley, P.M. (Eds.), Climate Change 2013: The Physical Science Basis. Contribution of Working Group I to the Fifth Assessment Report of the Intergovernmental Panel on Climate Change. Cambridge University Press, Cambridge, United Kingdom and New York, NY, USA.
IPCC, 2019. In: Shukla, P.R., Skea, J., Calvo Buendia, E., Masson-Delmotte, V., Pörtner, H.-O., Roberts, D.C., Zhai, P., Slade, R., Connors, S., van Diemen, R., Ferrat, M., Haughey, E., Luz, S., Neogi, S., Pathak, M., Petzold, J., Portugal Pereira, J., Vyas, P., Huntley, E., Kissick, K., Belkacemi, M., Malley, J. (Eds.), Climate Change and Land: an IPCC Special Report on Climate Change, Desertification, Land Degradation, Sustainable Land Management, Food Security and Greenhouse Gas Fluxes in Terrestrial Ecosystems. In press.
Kristensen, K., Schelde, K., Olesen, J.E., 2011. Winter wheat yield response to climate variability in Denmark. J. Agric. Sci. 149, 33–47. https://doi.org/10.1017/S0021859610000675.
Kronenberg, L., Yu, K., Walter, A., Hund, A., 2017. Monitoring the dynamics of wheat stem elongation: genotypes differ at critical stages. Euphytica 213, 157. https://doi.org/10.1007/s10681-017-1940-2.
Liu, B., Liu, L., Tian, L., Cao, W., Zhu, Y., Asseng, S., 2014. Post-heading heat stress and yield impact in winter wheat of China. Glob. Change Biol. 20, 372–381. https://doi.org/10.1111/gcb.12442.
Lobell, D.B., Schlenker, W., Costa-Roberts, J., 2011. Climate trends and global crop production since 1980. Science 333, 616–620. https://doi.org/10.1126/science.1204531.
Mäkinen, H., Kaseva, J., Trnka, M., Balek, J., Kersebaum, K.C., Nendel, C., Gobin, A., Olesen, J.E., Bindi, M., Ferrise, R., Moriondo, M., Rodríguez, A., Ruiz-Ramos, M., Takáč, J., Bezák, P., Ventrella, D., Ruget, F., Capellades, G., Kahiluoto, H., 2018. Sensitivity of European wheat to extreme weather. Field Crops Res. 222, 209–217. https://doi.org/10.1016/j.fcr.2017.11.008.
McMaster, G.S., Wilhelm, W.W., 2003. Phenological responses of wheat and barley to water and temperature: improving simulation models. J. Agric. Sci. 141, 129–147. https://doi.org/10.1017/S0021859603003460.
Meehl, G.A., Tebaldi, C., 2004. More intense, more frequent, and longer lasting heat waves in the 21st century. Science 305, 994–997. https://doi.org/10.1126/science.1098704.
Mondal, S., Singh, R.P., Mason, E.R., Huerta-Espino, J., Autrique, E., Joshi, A.K., 2016. Grain yield, adaptation and progress in breeding for early-maturing and heat-tolerant wheat lines in South Asia. Field Crops Res. 192, 78–85. https://doi.org/10.1016/j.fcr.2016.04.017.
Olesen, J.E., Børgesen, C.D., Elsgaard, L., Palosuo, T., Rötter, R.P., Skjelvåg, A.O., Peltonen-Sainio, P., Börjesson, T., Trnka, M., Ewert, F., Siebert, S., Brisson, N., Eitzinger, J., van Asselt, E.D., Oberforster, M., van der Fels-Klerx, H.J., 2012. Changes in time of sowing, flowering and maturity of cereals in Europe under climate change. Food Addit. Contam. A 29, 1527–1542. https://doi.org/10.1080/19440049.2012.712060.
Porter, J.R., Gawith, M., 1999. Temperatures and the growth and development of wheat: a review. Eur. J. Agron. 10, 23–36. https://doi.org/10.1016/S1161-0301(98)00047-1.
Price, K.V., Storn, R.M., Lampinen, J.A., 2006. Differential Evolution - a Practical Approach to Global Optimization. Berlin Heidelberg, Springer-Verlag. ISBN: 3540209506.
R Core Team, 2019. R: a language and environment for statistical computing. R Foundation for Statistical Computing, Vienna, Austria. https://www.R-project.org/.
Ren, S., Qin, Q., Ren, H., 2019. Contrasting wheat phenological responses to climate change in global scale. Sci. Total Environ. 665, 620–631. https://doi.org/10.1016/j.scitotenv.2019.01.394.
Rezaei, E.E., Siebert, S., Ewert, F., 2015. Intensity of heat stress in winter wheat—phenology compensates for the adverse effect of global warming. Environ. Res. Lett. 10, 024012 https://doi.org/10.1088/1748-9326/10/2/024012.
Rezaei, E.E., Siebert, S., Huging, H., Ewert, F., 2018. Climate change effect on wheat phenology depends on cultivar change. Sci. Rep. 8, 1–10. https://doi.org/10.1038/s41598-018-23101-2.
Richner, W., Sinaj, S., 2017. Grundlagen für die Düngung landwirtschaftlicher Kulturen in der Schweiz (GRUD 2017). Spezialpublikation, Agrarforsch. Schweiz 8, 276.
Rummukainen, M., 2012. Changes in climate and weather extremes in the 21st century. Wiley Interdiscip. Rev. Clim. Change 3, 115–129. https://doi.org/10.1002/wcc.160.
Saebo, A., Mortensen, L.M., 1996. Growth, morphology and yield of wheat, barley and oats grown at elevated atmospheric CO2 concentration in a cool, maritime climate. Agric. Ecosyst. Environ. 57, 9–15. https://doi.org/10.1016/0167-8809(95)01009-2.
Schär, C., Vidale, P.L., Lüthi, D., Frei, C., Häberli, C., Liniger, M.A., Appenzeller, C., 2004. The role of increasing temperature variability in European summer heatwaves. Nature 427, 332–336. https://doi.org/10.1038/nature02300.
Semenov, M.A., 2009. Impacts of climate change on wheat in England and Wales. J. R. Soc. Interface 6, 343–350. https://doi.org/10.1098/rsif.2008.0285.
Semenov, M.A., Shewry, P.R., 2011. Modelling predicts that heat stress, not drought, will increase vulnerability of wheat in Europe. Sci. Rep. 1, 1–5. https://doi.org/10.1038/srep00066.
Semenov, M.A., Stratonovitch, P., Alghabari, F., Gooding, M.J., 2014. Adapting wheat in Europe for climate change. J. Cereal Sci. 59, 245–256. https://doi.org/10.1016/j.jcs.2014.01.006.
Senepati, N., Semenov, M.A., 2020. Large genetic yield potential and genetic yield gap estimated for wheat in Europe. Glob. Food Sec. 24, 100340 https://doi.org/10.1016/j.gfs.2019.100340.
Seneviratne, S.I., Luthi, D., Litschi, M., Schar, C., 2006. Land-atmosphere coupling and climate change in Europe. Nature 443, 205–209. https://doi.org/10.1038/nature05095.
Shpiler, L., Blum, A., 1986. Differential reaction of wheat cultivars to hot environments. Euphytica 35, 483–492. https://doi.org/10.1007/BF00021856.
Slafer, G.A., Rawson, H.M., 1994. Sensitivity of wheat phasic development to major environmental factors: a re-examination of some assumptions made by physiologists and modellers. Funct. Plant Biol. 21, 393–426. https://doi.org/10.1071/PP9940393.
Slafer, G.A., Rawson, H.M., 1995. Development in wheat as affected by timing and length of exposure to long photoperiod. J. Exp. Bot. 46, 1877–1886. https://doi.org/10.1093/jxb/46.12.1877.
Springer, C.J., Ward, J.K., 2007. Flowering time and elevated atmospheric CO2. New Phytol. 176, 243–255. https://doi.org/10.1111/j.1469-8137.2007.02196.x.
Stratonovitch, P., Semenov, M.A., 2015. Heat tolerance around flowering in wheat identified as a key trait for increased yield potential in Europe under climate change. J. Exp. Bot. 66, 3599–3609. https://doi.org/10.1093/jxb/erv070.
Streck, N.A., Weiss, A., Baenziger, P.S., 2003a. A generalized vernalization response function for winter wheat. Agron. J. 95, 155–159. https://doi.org/10.2134/agronj2003.1550a.
Streck, N.A., Weiss, A., Xue, Q., Baenziger, P.S., 2003b. Improving predictions of developmental stages in winter wheat: a modified Wang and Engel model. Agric. For. Meteorol. 115, 139–150. https://doi.org/10.1016/S0168-1923(02)00228-9.
Strer, M., Svoboda, N., Herrmann, A., 2018. Abundance of adverse environmental conditions during critical stages of crop production in Northern Germany. Environ. Sci. Eur. 30, 1–16. https://doi.org/10.1186/s12302-018-0138-0.
Tao, F., Zhang, S., Zhang, Z., 2012. Spatiotemporal changes of wheat phenology in China under the effects of temperature, day length and cultivar thermal characteristics. Eur. J. Agron. 43, 201–212. https://doi.org/10.1016/j.eja.2012.07.005.
Torriani, D.S., Calanca, P., Schmid, S., Beniston, M., Fuhrer, J., 2007. Potential effects of changes in mean climate and climate variability on the yield of winter and spring crops in Switzerland. Climate Research 34, 59–69. https://doi.org/10.3354/cr034059.
Trnka, M., Rötter, R.P., Ruiz-Ramos, M., Kersebaum, K.C., Olesen, J.E., Žalud, Z., Semenov, M.A., 2014. Adverse weather conditions for European wheat production will become more frequent with climate change. Nat. Clim. Change 4, 637–643. https://doi.org/10.1038/nclimate2242.
Wang, E., Engel, T., 1998. Simulation of phenological development of wheat crops. Agric. Syst. 58, 1–24. https://doi.org/10.1016/S0308-521X(98)00028-6.
Wang, B., Liu, D.L., Asseng, S., Macadam, I., Yu, Q., 2015. Impact of climate change on wheat flowering time in eastern Australia. Agric. For. Meteorol. 209, 11–21. https://doi.org/10.1016/j.agrformet.2015.04.028.
Wardlaw, I.F., Blumenthal, C., Larroque, O., Wrigley, C.W., 2002. Contrasting effects of chronic heat stress and heat shock on kernel weight and flour quality in wheat. Funct. Plant Biol. 29, 25–34. https://doi.org/10.1071/PP00147.
Wickham, H., 2016. ggplot2: Elegant Graphics for Data Analysis. Springer-Verlag, New York.
Wu, L., Feng, L., Zhang, Y., Gao, J., Wang, J., 2017. Comparison of five wheat models simulating phenology under different sowing dates and varieties. Agron. J. 109, 1280–1293. https://doi.org/10.2134/agronj2016.10.0619.
Xue, Q., Weiss, A., Baenziger, P.S., 2004. Predicting phenological development in winter wheat. Climate Research 25, 243–252. https://doi.org/10.3354/cr025243.
Yip, S., Ferro, C.A.T., Stephenson, D.B., Hawkins, E., 2011. A simple, coherent framework for partitioning uncertainty in climate predictions. J. Clim. 24, 4634–4643. https://doi.org/10.1175/2011JCLI4085.1.
Zadoks, J.C., Chang, T.T., Konzak, C.F., 1974. A decimal code for the growth stages of cereals. Weed Res. 14, 415–421.